Thermal Analysis of Moving Wet Porous Longitudinal Exponential Fin in Hybrid Nanofluid by AGM and RKF45 Methods

Ramashree C R[1], Jyothi M V[2], Kousalya N[3], Rekha H B[4], Rakshitha M[5], Roopa Bai V R[6]
[1]*Post Graduate Department of Mathematics, The National College, Jayanagar, Bengaluru, Karnataka, India 560070.*

***Abstract*—The principal focus of this work is to examine the transfer of heat and steady state thermal distribution inside an exponentially profiled longitudinal moving permeable fin completely immersed in hybrid nanoliquid. The transmission of heat in the fin originates from the combination of conduction, convection, and radiation. The governing non linear ordinary differential equation that describes the associated fin problem is modeled using the Darcy model and the Fourier law of heat conduction. The developed equation is further reduced to a dimensionless equation with an appropriate boundary condition by using nondimensional terms. The Akbari Ganji method is used to solve the resulting nonlinear dimensionless problem semi analytically. Through a graphical representation, the impact of variable thermal factors on thermal behavior is investigated. The temperature distribution will be significantly impacted by the wet surface condition caused by the hybrid nature of nano liquids and the porous nature of the moving exponential fin, according to the results of this experiment. After comparing the resulting AGM findings with the numerical approach RKF 45, a high degree of consistency is found.**

***Index Terms*—Wet porous fin, Exponential profile, Hybrid nanofluid, AGM, RKF 45**

I. INTRODUCTION

Heat is primarily transferred by conduction, convection, and radiation. Many engineering applications, such as air conditioners, electronic processors, steam superheating units, energy transfer devices, combustion turbines, automotive heat exchangers, cooling systems, combustion chambers, energy recovery units, etc., require high heat transfer rates at low prices and sizes. In order to increase the heat transfer rate, the extended surface is added to the primary surfaces, called fins. Over the past few decades, several researchers have worked on this topic by considering different fin profiles in order to increase performance. Maji et al. [1] investigated how fins of various kinds could improve heat transfer while taking varying thermophysical and geometrical factors into account. Dogonchi et al. [2] examined the convection radiation heat transfer and heat creation that occurred simultaneously through a moving fin. In the automotive and aerospace industries, longitudinal fins are frequently employed to boost convection, which accelerates heat transfer between a base and air. Transient heat transfers in longitudinal fins for a range of profiles, such as rectangular, parabolic, convex, exponential, sinusoidal, and cosine profiles, has been studied by Navid Namdari et al. [3]. Although convective heat transmission can be effectively improved by conventional longitudinal fins, under certain operating conditions, adding porosity offers further thermal benefits. Heat interacts with the pores of a porous fin because its solid surface is instantly exposed to the surroundings. One of the major advantages of porous media fins is their increased effective surface area, which enables the fin to transfer heat to the working fluid. The convective heat transfer coefficient, radiation effect, internal thermal production, variability, and enthalpy flow of porous fins for the three common geometries longitudinal, spine, and annular disk have all been studied by Balaram Kundu and Se Jin Yook [4]. Mehrizi et al. [5] examined the impact of fin position and porosity on improving heat transmission in a plate porous media heat exchanger. Gireesha et al. [6] has investigated the thermal performance of a longitudinal profile's inclined porous fin. The wet situation is another effective way to increase the rate of heat transmission. Wet conditions are caused by the fluid that surrounds the fin. As a result, the fully moist condition has received a lot of attention, prompting the completion of various studies. Hatami et al. [7] modeled the thermal performance of a completely wetted porous fin with a semi spherical profile, whereas the mass and heat transfer efficiency of a fully wet exponential and a straight porous fins were evaluated by Turkyilmazoglu [8], and he found that the exponential porous fin outperforms the straight porous fin. Using the spectral colocation approach with natural convection and radiation, Darvishi et al. [9] has studied the thermochemical study of a fully wet porous radial fin. The thermal performance of a totally wet porous fin in a radial profile by using the finite element method was investigated by Gireesha et al. [10].

Additionally, continuous motion has been employed in several kinds of production processes, including extrusion, hot rolling, glass fiber designs, automobiles, and so on. Cooling is therefore required when moving continuously. Because of its wide usage, a moving fin is thus employed. Several researchers did a thermal investigation of the moving fin surface [11,12, 13, 14]. In a convective radiative environment, the improvement of heat transmission from a constantly moving porous fin has been studied by D Bhanja et al. [15]. Zia Ud Din et al. [16] looked into the combined effects of convection, porosity, and radiation as well as the moving exponential fin when internal heat generation was present and convective boundary conditions were in place. Gireesha et al. [17] have examined the temperature field of a moving longitudinal porous fin with varying internal heat generation with respect to temperature under the effects of convection and natural radiation.

Furthermore, in order to improve overall heat transfer performance and complement moving fin systems, recent developments in thermal management have concentrated on integrating sophisticated working fluids, such as nanofluids. Nanofluids, which are novel heat transfer fluids created by suspending nanoscale particles into typical base fluids, have attracted widespread interest in thermal management systems because they possess higher heat transfer performance. Nanofluids are employed as coolants in several industries, including automotive, aerospace, and electronics. Many attempts to create nanofluids have employed either a single step physical method that simultaneously creates and disperses the nanoparticles into base fluids [18, 19, 20] or a two step method that first creates nanoparticles and then disperses them into base fluids [21, 22].

Nanofluids have higher thermal conductivity which leads to improved heat transfer performance and lower energy usage. The global thermal response of nanofluids is determined by a number of factors, including nanoparticle type, diameter, shape, and concentration, suspension stability, and operating temperature. Khalaf et al. [23] studied the enhancement of heat transfer by the use of porous media, nanoliquid, and fins. Whereas, the hybrid nanofluids have been created by combining two or more different nanoparticles in an effort to further enhance heat transfer characteristics. HVAC systems, natural convection enclosures, heat exchangers, heat sinks, heat pipes, jet impingement cooling, boiling, and latent heat thermal energy storage systems all use hybrid nanofluids. In comparison to a single or mono nanoparticle in the base fluid, Dhinesh Kumar et al. [24] found that a hybrid nanofluid offers a superior enhancement in thermophysical properties, particularly in thermal conductivity. The importance of hybrid nanofluid in improving heat transmission was examined by Srinivasan et al. [25]. Thermal analysis for the radiative convective exponential porous fin wetted with $TiO_2 - SiO_2$/hexanol hybrid nanofluid has been studied by Amal Abdulrahman et al. [26]. In the presence of natural convection and heat radiation, Gireesha et al. [27] uses computational methods to examine the flow of nanoparticle infused water based hybrid nanoliquid across a permeable longitudinal fin moving at a constant speed. Gireesha et al. [28] investigated that MWCNTs have superior heat transmission compared to SWCNTs. Selvam et al. [29] studied the convective heat transfer properties of a water ethylene glycol combination containing silver nanoparticles. Gireesha et al. [30] explored the flow of a hybrid nanofluid with natural convection and thermal radiation across a permeable longitudinal moving fin. The effect of ethylene glycol as a material that shifts phases in a cold storage unit on cooling retention has been studied by Krishna Kumar Gupta et al. [31]. He came to the conclusion that a composition of 50% water and 50% ethylene glycol offer good cooling stability.

AGM is a very accurate and efficient analytical technique for resolving highly nonlinear differential equations. Additionally, the Runge Kutta Fehlberg fourth fifth order method is employed to solve the modified non dimensional zed ordinary differential equation. The heat transfer of a porous fin in a specific thermal non equilibrium condition was investigated by Jalili et al. [32] using AGM and other numerical methods. By using the AGM approach analytically and the Range Kutta technique numerically, Ganji et al. [33] examine the heat transfer analysis of a fin with temperature dependent thermal conductivity and heat transfer coefficient. Mirgolbabaee et al. [34] examine a numerical comparison between the Range Kutta Method and a semi analytical Akbari Ganji's method approach for solving nonlinear oscillators. Ganji et al. [35] studied the numerical comparison of the Range Kutta Method and the analysis of the nonlinear heat transfer problem using AGM. Sowmya et al. [36] examined natural convection and radiation in a fully wetted longitudinal permeable fin with combined variation of surface emissivity, coefficient of heat transfer, and thermal conductivity with temperature by applying a Runge Kutta Fehlberg fourth fifth order method based on the shooting technique.

Keeping all of these aspects in mind, we want to examine the thermal behavior of the longitudinally moving exponential profile fin immersed in the $Ag-$ MWCNT/ethylene glycol + water hybrid nanofluid under the influence of natural convection and radiation. In the present study, we use MWCNT and Ag as nanoparticles and ethylene glycol+water $(50\% + 50\%)$ as a base fluid because,

- MWCNTs have superior heat transmission, and Ag has the best heat transfer properties.
- 50% water and 50% ethylene glycol provide good cooling retention.

II. FORMATION OF MSTHEMATICAL CONCEPT

The graphic depicts a physical model of the current analysis. Let us consider a longitudinal wet porous fin of length L and thickness $2t_b$ with a moving exponential profile. The preliminary surface on which the fin is affixed has a temperature T_b. Natural convection and radiation cause heat losses to the surrounding nanofluids, whereas conduction transfers heat from the main surface to the fin tip. Because the fin's exposed surface discharges radiation into the nanofluid, the environment around the nanofluid also serves as a radiative sink. The following assumptions are made for simplicity:

- The fin's surface is influenced by radiation and convection, and their cross section area varies with the $t(x)$ function.
- In order to model the current thermal analysis, it is assumed that the surrounding temperatures are constant, the fin
- substance is isotropic, and the surface emissivity is influenced by temperature.
- The fluid and the moving wet porous media interact according to Darcy's law.
- It is supposed to be the coefficient of convective heat transmission, which is nonlinear.
- The fin is presumed to be completely saturated with $Ag-$ MWCNT/ethylene glycol+water hybrid nanofluid.

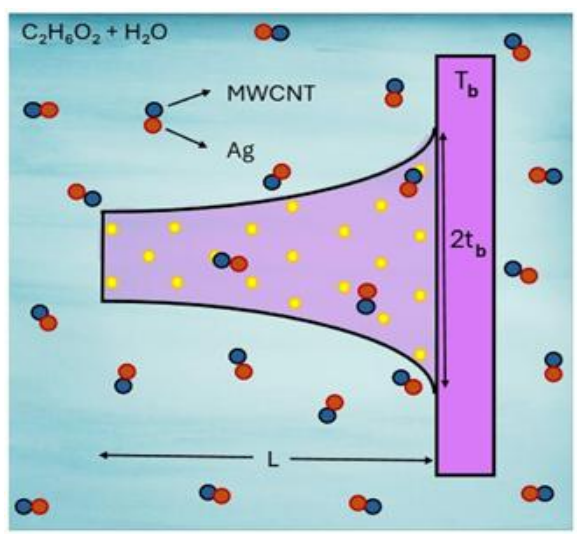

Figure 1: Physical representation of a nanofluid flowing across an exponentially porous fin

The governing steady state energy balance equation is as follows:

$$\bar{Q}(x) - \bar{Q}(x+dx) = (1-\phi)h^*(T)(T-T_a)W\,dx + h_R i_{fg}(1-\phi)(\omega-\omega_a)Wdx - (\rho C_p)_{hnf}\, t(x)U\frac{dT}{dx}Wdx + \dot{m}C_{p_{hnf}}(T-T_a) + \varepsilon^*(T)\sigma F_{f-a}(T^4-T_a^4)W\,dx \quad (1)$$

The heat transfer rate in the present instance is Q(x), which can be described by Fourier's rule of conduction which is as follows:

$$\overline{Q}(x) = -k_{hnf}Wt(x)\frac{dT}{dx} \quad (2)$$

The fluid's mass flow rate through a porous medium can be described using the following method

$$\dot{m} = \rho_{hnf}v(x)Wdx \quad (3)$$

The Darcy's model specifies the passage velocity $v(x)$, that corresponds to

$$\upsilon(x) = \frac{gK\beta_{hnf}(T-T_a)}{\upsilon_{hnf}} \quad (4)$$

The emissivity $\varepsilon^*(T)$ and temperature dependent convective heat transfer coefficient $h^*(T)$ can be obtained as

$$h^*(T) = h_a\left[\frac{T-T_a}{T_b-T_a}\right]^m = h_R C_{p_{hnf}} Le^{\frac{2}{3}} \quad (5)$$

$$\varepsilon^*(T) = \varepsilon_a\left[1+\alpha\left(\frac{T-T_a}{T_b-T_a}\right)\right] \quad (6)$$

The fluctuation in fin thickness over its elongated length determines the fin profile, and the local fin thickness with the porous fin component is displayed as

$$t(x) = t_b e^{\gamma\left(\frac{x}{L}-1\right)} \quad (7)$$

By assuming the above equations, the eq. (1) will becomes,

$$R_1\frac{d}{dx}\left[e^{\gamma\left(\frac{x}{L}-1\right)}\frac{dT}{dx}\right] = \frac{(\rho C_p)_f gk(\rho\beta)_f}{\mu_f t_b k_f}\frac{R_2R_3}{R_4}(T-T_a)^2 + \frac{h_a}{t_b k_f}(1-\varphi)\frac{(T-T_a)^{m+1}}{(T_b-T_a)^m} + \frac{h_a i_{fg}}{t_b k_f (C_p)_f Le^{\frac{2}{3}}}(1-\varphi)\left[\frac{T-T_a}{T_b-T_a}\right]^m(\omega-\omega_a)^2 + \frac{\varepsilon_a\sigma F_{f-a}}{t_b k_f}\left[1+\alpha\left(\frac{T-T_a}{T_b-T_a}\right)\right](T^4-T_a^4) - \frac{(\rho C_p)_f U}{k_f}e^{\gamma\left(\frac{x}{L}-1\right)}\frac{dT}{dx}R_2$$

Table 1: Thermophysical properties of Ag, MWCNT, and $C_2H_6O_2$ (50%) + H_2O (50%)

Thermophysical Properties	Ag	MWCNT	$C_2H_6O_2 + H_2O$
ρ (kgm^{-3})	10490	1600	1063.8
C_p ($Jkg^{-1}K^{-1}$)	235	796	3630
k ($Wm^{-1}K^{-1}$)	429	3000	0.387
β (K^{-1}) $\times 10^{-5}$	1.89	44	5.8

The thermophysical properties of nanofluid under consideration are mathematically addressed as: [37]

$$R_1 = \frac{k_{hnf}}{k_f} = \left[\frac{2k_{nf}+k_{s_2}+(k_{s_2}-k_{nf})2\varphi_2}{2k_{nf}+k_{s_2}-\varphi_2(k_{s_2}+k_{nf})}\right]\left[\frac{k_{s_1}+2k_f-2\varphi_1(k_f-k_{s_1})}{k_{s_1}+2k_f+\varphi_1(k_f-k_{s_1})}\right]$$
$$R_2 = \frac{(\rho C_p)_{hnf}}{(\rho C_p)_f} = \left[(1-\varphi_1)\frac{(\rho C_p)_{s_1}}{(\rho C_p)_f}+\varphi_1\right](1-\varphi_2)+\varphi_2\frac{(\rho C_p)_{s_2}}{(\rho C_p)_f}$$
$$R_3 = \frac{(\rho\beta)_{hnf}}{(\rho\beta)_f} = \left[(1-\varphi_1)\frac{(\rho\beta)_{s_1}}{(\rho\beta)_f}+\varphi_1\right](1-\varphi_2)+\varphi_2\frac{(\rho\beta)_{s_2}}{(\rho\beta)_f}$$
$$R_4 = \frac{\mu_{hnf}}{\mu_f} = \frac{1}{(1-\varphi_1)^{2.5}(1-\varphi_2)^{2.5}} \quad (9)$$

The required adiabatic boundary conditions are given by

$$T = T_b \text{ at } x = L$$
$$\frac{dT}{dx} = 0 \text{ at } x = 0 \quad (10)$$

Dimensionless parameters are included to the previously mentioned equations to make them less complicated.

$$T(x) = T_b\theta(x),\ T_a = T_b\theta_a,\ X = \frac{x}{L},\ N_{cc} = \frac{h_aL^2}{t_bk_f},$$
$$P_s = \frac{(\rho C_p)_f gK(\rho\beta)_f L^2T_b}{\mu_f t_b k_f},\ \ Pe = \frac{L(\rho C_p)_f U}{k_f},\ \psi = \frac{h_a i_f g b_2 L^2}{t_b k_f (C_p)_f Le^{\frac{2}{3}}},$$
$$N_{cr} = \frac{\epsilon_a\sigma F_{f-a}L^2T_b^3}{t_bk_f},\ \omega-\omega_a = b_2(T-T_a) \quad (11)$$

Utilizing eq. (11), eq. (8) becomes

$$R_1 e^{\gamma(X-1)} \frac{d^2\theta}{dX^2} + R_1 e^{\gamma(X-1)} \frac{d\theta}{dX} = P_s \frac{R_2 R_3}{R_4} (\theta - \theta_a)^2 + N_{cc}(1-\phi) \frac{(\theta-\theta_a)^{m+1}}{(1-\theta_a)^m} + \psi(1-\phi) \frac{(\theta-\theta_a)^{m+1}}{(1-\theta_a)^m} - Pe\, e^{\gamma(X-1)} \frac{d\theta}{dX} R_2 + N_{cr}[1+\alpha\left(\frac{\theta-\theta_a}{1-\theta_a}\right)](\theta^4 - \theta_a^4) \quad (12)$$

Here are the reduced boundary conditions:

$$\theta = 1 \text{ at } X = 1, \quad \frac{d\theta}{dX} = 0 \text{ at } X = 0 \quad (13)$$

III. COMPUTATIONAL METHODS

1 Akbari Ganji's Method (AGM)

The Akbari Ganji's Method is a semi analytical approach to solving non-linear differential equations which was invented by D.D. Ganji. The generalized form of the differential equation solved by AGM is provided by

$$Pk: G(y, y', y'', y''', \ldots, y^{(m)}) = 0 \quad (14)$$

The nonlinear differential equation of p, a function of y, and the parameter y, a function of z, where m is the order of the highest derivative and $y = y(z)$ is the function to be determined. The technique expresses the solution as a polynomial series and subsequently uses the boundary conditions for determining the unknown coefficients. Boundary conditions:

At $z = 0$,

$$y(0) = y_0, y'(0) = y_0', \; y''(0) = y_0'', y'''(0) = y_0''', \ldots, y^{(m)}(0) = y_0^{(m)}$$

At $z = L$,

$$y(L) = y_L, y'(L) = y_L', y''(L) = y_L'', y'''(L) = y_L''', \ldots, y^{(m)}(L) = y_L^{(m)} \quad (15)$$

The following are the basic steps in the Akbari Ganji method:

Step 1: Assume a Polynomial Series Solution: The process begins by assuming that there is a polynomial series solution for the dependent variable y(z) as

$$y(z) = \sum_{i=0}^{m} b_i z^i = b_0 + b_1 z + b_2 z^2 + \cdots + b_m z^m \quad (16)$$

The unknown coefficients that must be found in this case are b_i.

Step 2: Apply Boundary Conditions to the Assumed Solution: Now apply boundary conditions to the assumed solution:

At $z = 0$,

$$\begin{cases} y(0) = b_0 = y_0 \\ y'(0) = b_1 = y_0' \\ y''(0) = 2b_2 = y_0'' \\ \vdots \quad \vdots \quad \vdots \end{cases}$$

At $z = L$,

$$\begin{cases} y(L) = b_0 + b_1 L + \cdots + b_m L^m = y_L \\ y'(L) = b_1 + 2b_2 L + \cdots + m b_m L^{m-1} = y_L' \\ y''(L) = 2b_2 + 6b_2 L + \cdots + m(m-1) b_m L^{m-2} = y_L'' \\ \vdots \quad \vdots \quad \vdots \quad \vdots \quad \vdots \quad \vdots \quad \vdots \end{cases} \quad (17)$$

A collection of equations involving the unknown coefficients b_i is produced by these applications.

Step 3: Generate Additional Equations from the Governing Differential Equation: Next, we apply the boundary conditions to the governing differential equation. These boundary conditions are directly used with the original differential equation and its higher order derivatives to create additional equations. These new equations are necessary to solve for the unknown coefficients. This process involves evaluating the differential equation at the boundary points, which are ($z = 0$ and $z = L$).

For the original equation,

$$G(y, y', y'', y''', \ldots, y^{(m)}) = 0 \quad (18)$$

At $z = 0$,

$$G\left(y(0), y'(0), y''(0), y'''(0), \ldots, y^{(m)}(0)\right) = 0$$

At $z = L$

$$G\left(y(L), y'(L), y''(L), y'''(L), \ldots, y^{(m)}(L)\right) = 0 \quad (19)$$

Higher order derivatives of the governing equation (G', G'', etc.) are taken with respect to z if additional equations are required, and the boundary conditions are also applied to these expressions.

For example:

$$G'(y, y', \ldots, y^{m+1}) = 0$$

$$G'\left(y(0), y'(0), \ldots, y^{(m+1)}(0)\right) = 0 \text{ At } z = 0,$$

$$G'\left(y(L), y'(L), \ldots, y^{m+1}(L)\right) = 0 \; At \; z = L.$$

Step 4: Solve the System of Algebraic Equations: A system of $(m + 1)$ algebraic equations for the $(m + 1)$ unknown coefficients $(b_0, b_1, \ldots, b_m)$ can be generated through the addition of the equations from Steps 2 and 3. The values for these coefficients can be determined by solving this system, providing the approximate analytical solution to the nonlinear differential equation.

Step 5: Substitute Coefficients into the Assumed Solution: Once the values of $b_0, b_1, \ldots, b_m$ are determined from Step 4, substitute them back into the assumed polynomial series solution from Step 1:

$$y(z) = b_0 + b_1 z + b_2 z^2 + \cdots + b_m z^m$$

This $y(z)$ represents the approximate analytical solution to the given nonlinear differential equation.

2 Runge Kutta Fehlberg Method (RKF 45)

Initial value problems (I.V.P.s) can be solved more quickly and precisely with the adaptive numerical methodology known as the Runge Kutta Fehlberg method (RKF45) than with more straightforward methods. It streamlines the process by computing two approximations for the solution at each step, improving upon the simple method of solving a problem twice with step sizes h and $\frac{h}{2}$.

Simultaneously computing a fourth order and a fifth order approximation is the main concept. The inaccuracy is estimated from the difference between these two approximations. To maintain a specified level of precision, the approach adaptively modifies the step size (h) for the subsequent iteration based on this inaccuracy.

Steps of the RKF45 Method

A. Calculate Six Intermediate Values (l_1 to l_6): At each step, the following six parameters are determined using the differential equation function $f(t, y)$ and the present step size h:

$$l_1 = hf(t_k, y_k)$$

$$l_2 = hf\left(t_k + \frac{1}{4}h, y_k + \frac{1}{4}l_1\right)$$

$$l_3 = hf\left(t_k + \frac{3}{8}h, y_k + \frac{3}{32}l_1 + \frac{9}{32}l_2\right)$$

$$l_4 = hf\left(t_k + \frac{12}{13}h, y_k + \frac{1932}{2197}l_1 - \frac{7200}{2197}l_2 + \frac{7296}{2197}l_3\right)$$

$$l_5 = hf\left(t_k + h, y_k + \frac{439}{216}l_1 - 8l_2 + \frac{3680}{513}l_3 - \frac{845}{4104}l_4\right)$$

$$l_6 = hf\left(t_k + \frac{1}{2}h, y_k - \frac{8}{27}l_1 + 2l_2 - \frac{3544}{2565}l_3 + \frac{1859}{4104}l_4 - \frac{11}{40}l_5\right)$$

B. Compute Two Approximations for the Next Solution: Two distinct approximations for the solution are calculated at the following step, y_{k+1}.

Fourth Order Approximation (y_{k+1}):

$$y_{k+1} = y_k + \frac{25}{216}l_1 + \frac{1408}{2565}l_3 + \frac{2197}{4101}l_4 - \frac{1}{5}l_5$$

The variables l_1, l_3, l_4, and l_5 are used in this formula. Keep in mind that this estimate does not require l_2.

Fifth Order Approximation (z_{k+1}):

$$z_{k+1} = y_k + \frac{16}{135}l_1 + \frac{6656}{12825}l_3 + \frac{28561}{56430}l_4 - \frac{9}{50}l_5 + \frac{2}{55}l_6$$

This formula uses l_1, l_3, l_4, l_5, and l_6.

C. Determine the New Step Size: An estimate of the inaccuracy is given by the difference between the two estimates, $|z_k + 1 - y_k + 1|$. To ascertain whether the solution is sufficiently exact, this error is compared to a predetermined tolerance (tol). The current step size h is then multiplied by a scalar s to determine the optimal step size for the following iteration, sh.

$$s = \left(\frac{tol\,.\,h}{2|z_{k+1} - y_{k+1}|}\right)^{1/4} \approx 0.84\left(\frac{tol\,.\,h}{2|z_{k+1} - y_{k+1}|}\right)^{1/4}$$

IV. RESULTS AND DISCUSSION

A parametric investigation has been done on the performance of a porous fin in fully wet conditions with radiation and natural convection with an exponential profile. The constant values are $N_{cc} = 1, N_{cr} = 1, \theta_a = 0.5$, and each parameter is changed while maintaining the others constant. $\gamma = 0$, $m = 0, P_s = 0.1, \psi = 1, Pe = 0.5, \phi = 0.03$ and $\alpha = 0.2$.

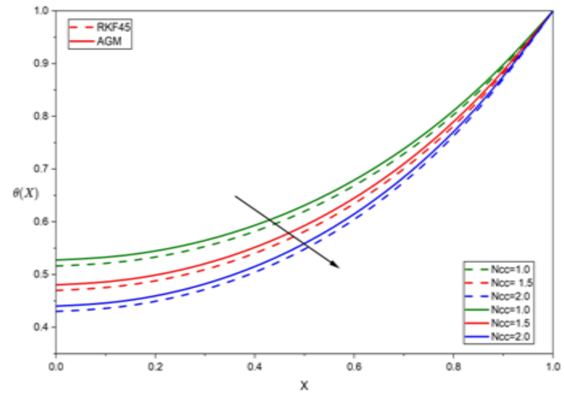

Figure 2: Variation in the distribution of temperature as N_{cc} values increase.

Figure 2 shows that as the N_{cc} increases, there will be more convection. More heat is consequently released into the surroundings by the fin. The thermal profile decreases and the fin cools more quickly as the convective parameter increases. The temperature profile declines as N_{cc} grows. This is evident from the fact that when the convection effect increases, more heat is transferred from the fin surface. Thus, the temperature of the fin decreases. The temperature decreases exponentially in the axial direction as the N_{cc} value rises.

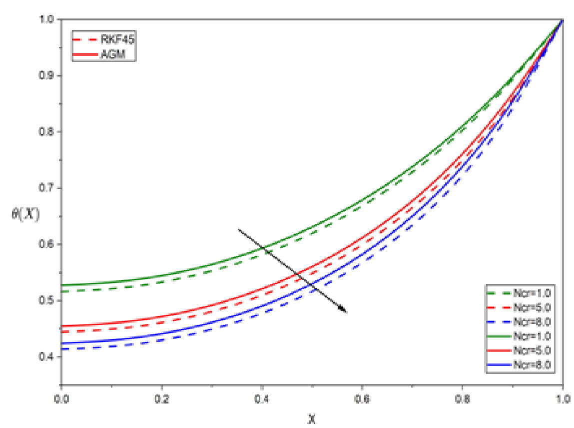

Figure 3: Variation in the distribution of temperature as N_{cr} values increase.

Figure 3 shows that the thermal profile reduces as the radiative parameter rises. This is because as the radiative parameter rises, the surface radiation rises as well, transmitting more heat from the fin's surface.

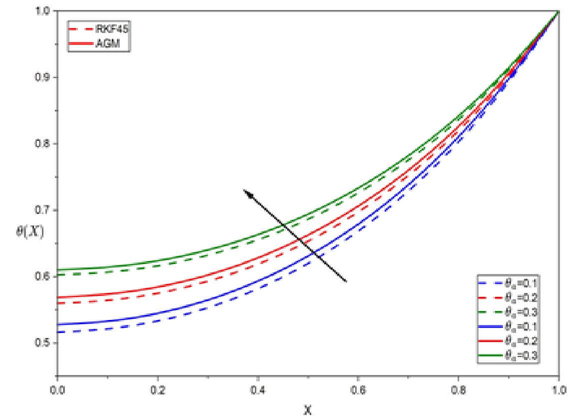

Figure 4: Variation in the distribution of temperature as θ_a values increase.

Figure 4 shows that higher ambient temperatures lead to an increase in the fin's temperature profile. The increase occurs because a warmer surrounding fluid reduces the rate of heat transfer from the fin's surface to its surroundings. Consequently, as the ambient temperature (θ_a) rises, the dimensionless temperature of the fin also increases, indicating less heat dissipation from the fin.

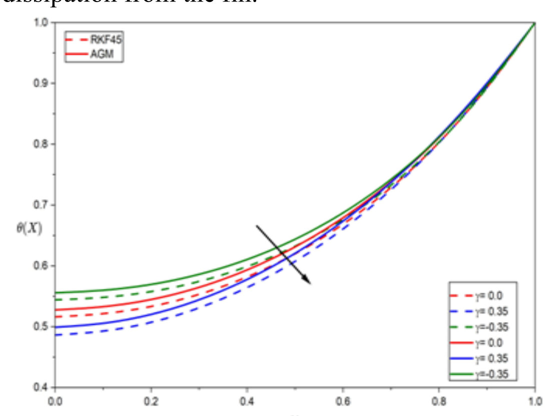

Figure 5: Variation in the distribution of temperature as γ values increase.

Figure 5 shows that the fin's temperature profile is nonlinear, meaning that it increases as the exponential power index γ does. It's crucial to remember that a case is nonlinear when γ values are greater than zero but linear when γ equals zero. The significance of γ in establishing the degree of nonlinearity is so illustrated. Then, γ has a significant impact on the fin structure's temperature distribution. A higher thermal profile corresponds directly with a higher power index. The temperature and heat transport characteristics of these fins are thus controlled by the power index.

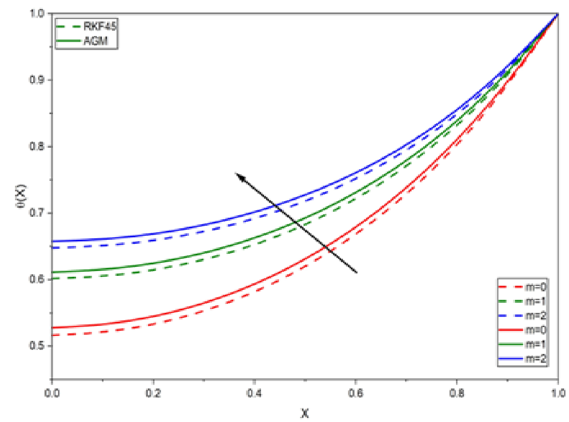

Figure 6: Variation in the distribution of temperature as m values increase.

Figure 6 shows that the fin's thermal profile rises as the power index m does, with varying values of m signifying different flow regimes. The growing relationship between temperature distribution and m is evident. A decreasing fin temperature is associated with lower values of m, but a more prominent thermal profile is caused by larger values of m. This suggests that the exponent m plays a direct role in determining the various flow regimes' characteristics by influencing the fin's heat distribution.

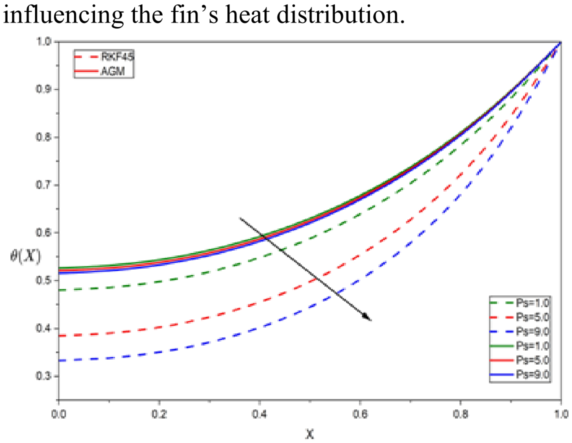

Figure 7: Variation in the distribution of temperature as P_s values increase.

Figure 7 shows that the effect of the porosity parameter on the thermal profile of the fin. As the porosity parameter increases, the fin's surface temperature decreases. This is due to the porosity parameter being a product of the Rayleigh and Darcy numbers. The greater the Rayleigh number, the higher the fin permeability, which enhances fluid infiltration through the fin pores. By increasing the buoyancy force impact, convection from the fin surface has been transmitted from the fin's surface and therefore increases as the porosity parameter increases.

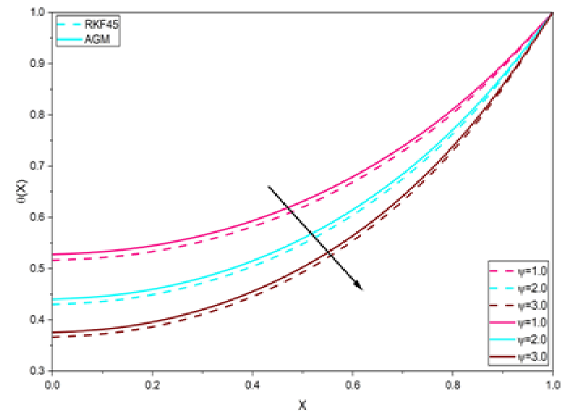

Figure 8: Variation in the distribution of temperature as ψ values increase.

Figure 8 shows that as the wet parameter increases, th e temperature gradient decreases due to the wet state s urrounding the fin. Because of the increased rate of he at transfer and greater absorption of heat from the fin surface, the fin cools down faster in this wet condition This also increases the efficiency of the fin.

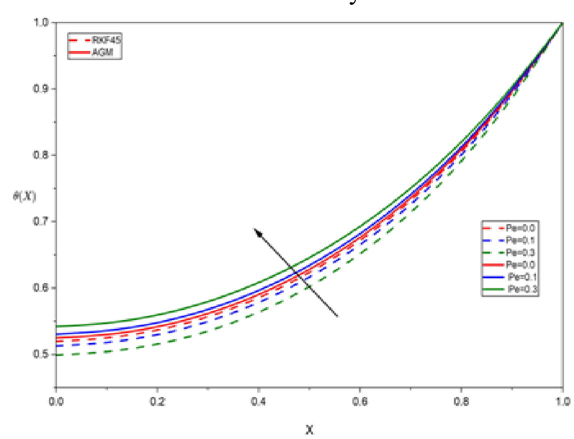

Figure 9: Variation in the distribution of temperature as Pe values increase.

Figure 8 shows that the fin temperature rises in proportion to the Pe. This is due to the fact that when Pe rises, the moving fin's velocity also does. Time decreases as velocity rises. to engage with both the fin and the surroundings. Because of this, the effect of the Peclet number (Pe) on the thermal performance diminishes as Pe grows. It is discovered that an increase in the temperature profile coincides with an increase in Pe. Physically, the ratio of the advective to diffuse transport rates is referred to as the Peclet number. There is less evaporation into the environment when the fin's temperature and speed grow with an increase in Peclet number.

V. CONCLUSION

The effects of radiation and convection on the thermal behavior of a moving longitudinal wet porous fin Ag + MWCNT/ethylene glycol+water hybrid nanoliquid have been investigated. In the current investigation, we have utilized AGM to determine the nonlinear heat transfer equation's approximate solutions in a longitudinal fin; the outcomes are contrasted with those obtained using the RKF 45 approach. We conducted a graphical evaluation of the effect of dimensionless parameters in the simplified equation. Some of the most significant results of the investigation are listed below.

- With rise in convective parameter N_{cc}, wet parameter ψ and radiative parameter N_{cr}, temperature distribution decreases.
- The temperature distribution rises as the peclet number Pe increases.
- With rise in ambient temperatures θ_a and power index m temperature distribution increases.
- Higher values Ps cause a rapid decrease in fin temperature.

VI. NOMENCLATURE

k	Thermal conductivity $[Wm^{-1}K^{-1}]$
K	Permeability $[m^{-2}]$
C_p	Specific heat capacity $[Jkg^{-1}K^{-1}]$
T_b	Fin base temperature
T_a	Fin ambient temperature
m	Thermal conductivity parameter
N_{cc}	Conduction convective parameter
N_{cr}	Conduction radiative parameter
h_R	Uniform mass transfer $[kgm^{-2}s^{-1}]$
L_e	Lewis number
Pe	Peclet number
i_{fg}	Latent heat of evaporation
h^*	Convective heat transfer coefficient
F_{f-a}	Shape factor for radiation heat transfer
L	Fin length [m]
g	Acceleration due to gravity $[ms^{-2}]$
$\bar{Q}$	Base heat flow
T	Temperature
P_s	Porous parameter
b_2	Variable parameter $[K^{-1}]$
h	Heat transfer coefficient
U	Uniform velocity of the fin
W	Fin width
$t(X)$	Fins semi thickness
w_a	Specific humidity
t_b	Semi base fins thickness
ϵ^*	Emissivity
θ	Non-Dimensional temperature
$\emptyset$	Porosity
γ	Exponential index parameter
ρ	Density $[kgm^{-3}]$
v	Kinematic viscosity
β	Thermal Expansion
σ	Stefan Boltzmann Constant
φ_1 and (	Nanoparticles volume fractions
φ	Wet parameter
μ	Dynamic viscosity $[kgm^{-1}s^{-1}]$

Subscript

f	Fluid
hnf	Hybrid nanofluid
a	Ambient
nf	Nanofluid
s_1 and s_2	Solid nanoparticles
b	Base

REFERENCES

[1] Khoram Nejad, E.S., Moradi, S., Shishehsaz, M., Effect of crack characteristics on the vibration behavior of post buckled functionally graded plates, Structures, 50, 181 199, 2023.

[2] A., Maji, G., Choubey, Improvement of heat transfer through fins: A brief review of recent developments, Heat Transfer, 49(3), pp 1658 1685, 2020.

[3] A.S., Dogonchi, D.D., Ganji, Convection–radiation heat transfer study of moving fin with temperature dependent thermal conductivity, heat transfer coefficient and heat generation, Applied thermal engineering, 103, pp 705 712, 2016.

[4] Navid Namdari, Morteza Abdi, Hamidreza Chaghomi, Farzad Rahmani, Numerical solution for transient heat transfer in longitudinal fins, International Research Journal of Advanced Engineering and Science, 3(2), pp 131 136, 2018.

[5] B., Kundu, S.J., Yook, an accurate approach for thermal analysis of porous longitudinal, spine

and radial fins with all nonlinearity effects–analytical and unified, Applied Mathematics and Computation, 402, 126124, 2021.

[6] A.A., Mehrizi, M., Farhadi, K., Sedighi, M.A., Delavar, Effect of fin position and porosity on heat transfer improvement in a plate porous media heat exchanger, Journal of the Taiwan Institute of Chemical Engineers, 44(3), 420431, 2013.

[7] B.J., Gireesha, G., Sowmya, Heat transfer analysis of an inclined porous fin using differential transform method, International Journal of Ambient Energy, 43(1), pp 3189 3195, 2022.

[8] M., Hatami, G.H.R.M., Ahangar, D.D., Ganji, K., Boubaker Refrigeration efficiency analysis for fully wet semi spherical porous fins, Energy conversion and management, Elsevier Ltd, 84, 533 540,2014.

[9] M., Turkyilmazoglu, Efficiency of heat and mass transfer in fully wet porous fins: exponential fins versus straight fins, international journal of refrigeration, Elsevier Science Inc., Volume 46, pp 158 164, 2014.

[10] F., Khani, M.T., Darvishi, R.S.R., Gorla, B.J., Gireesha, Thermal analysis of a fully wet porous radial fin with natural convection and radiation using the spectral collocation method. International Journal of Applied Mechanics and Engineering, 21(2), pp 377 392, 2016.

[11] G., Sowmya, B.J., Gireesha, O.D., Makinde, "Thermal performance of fully wet longitudinal porous fin with temperature dependent thermal conductivity, surface emissivity and heat transfer coefficient", Multidiscipline Modeling in Materials and Structures, Emerald Publishing Limited, 16(4), pp 749 764, 2020.

[12] B.J., Gireesha, G., Sowmya, S., Sindhu, Analysis of thermal behavior of moving longitudinal porous fin wetted with water based SWCNTs and MWCNTs, Heat Transfer, Wiley Periodicals Inc., 49(4), pp 2044 2058, 2020.

[13] T.S., Kumar, P.A., Dinesh, S.B., Ramakrishna, A.S., Reddy, Numerical study of moving fin with thermal properties, Heat Transfer, Wiley Periodicals Inc., 51(6), pp 5623 5634, 2022.

[14] I., Ullah, S., Ullah, A., Ali, S.I., Shah, W., Weera, M.M., Alam, Heat transfer analysis from moving convection radiative triangular porous fin exposed to heat generation. Case Studies in Thermal Engineering, Case Studies in Thermal Engineering, Elsevier Ltd., Volume 38, 2022.

[15] G., Sowmya, B.J., Gireesha, M., Madhu, Analysis of a fully wetted moving fin with temperature dependent internal heat generation using the finite element method, Heat Transfer, Wiley Periodicals Inc., 49(4), pp 1939 1954, 2020.

[16] D., Bhanja, B., Kundu, A., Aziz, Enhancement of heat transfer from a continuously moving porous fin exposed in convective–radiative environment, Energy Conversion and Management, Elsevier Ltd., pp 842 853, 2014.

[17] Zia Ud Din, Amir Ali, A., Zareen Khan, Gul Zaman, Heat transfer analysis: convective radiative moving exponential porous fins with internal heat generation, Mathematical Biosciences and Engineering, American Institute of Mathematical Sciences, 19(11), pp 11491 11511 2022.

[18] G., Sowmya, B.J., Gireesha, M., Madhu, Analysis of a fully wetted moving fin with temperature dependent internal heat generation using the finite element method, Heat Transfer, Wiley Periodicals Inc., 49(4), pp 1939 1954, 2020.

[19] S.U.S., Choi, J.A., Eastman, Enhanced heat transfer using nanofluids, Argonne National Laboratory (ANL), osti.gov, 2001.

[20] J.A., Eastman, S.U.S., Choi, S., Li, W., Yu, Anomalously Increased Effective Thermal Conductivities of Ethylene Glycol Based Nanofluids Containing Copper Nanoparticles, American Institute of Physics, 78(6), pp 718 – 720, 2001.

[21] M.M., Kostic, "Critical Issues and Application Potentials in Nanofluids Research", Proceedings of Multifunctional Nanocomposites, American Society of Mechanical Engineers, pp 191 199, 2006.

[22] S.U.S., Choi, Z. G., Zhang, P., Keblinski, 2004, Nanofluids: Encyclopedia of Nanoscience and Nanotechnology, H. S. Nalwa, ed., Vol. 6, American Scientific Publishers, New York, pp. 757–773.

[23] G.P., Peterson, C.H., Li, Heat and Mass Transfer in Fluids with Nanoparticle Suspensions,

Advances in Heat Transfer, Elsevier Ltd, Volume 39, pp 257 –376, 2006.

[24] A.F., Khalaf, A., Basem, H.Q., Hussein, A.K., Jasim, K.A., Hammoodi, A.M., Al Tajer, I., Omer, M.A., Flayyih, Improvement of Heat Transfer by Using Porous Media, Nanofluid, and Fins: A Review, International Journal of Heat & Technology, 40(2), pp 497 521, 2022.

[25] D.D., Kumar, A.V., Arasu, A comprehensive review of preparation, characterization, properties and stability of hybrid nanofluids, Renewable and Sustainable Energy Reviews, Elsevier Ltd., Volume 81, 1669 1689, 2018.

[26] M., Muneeshwaran, G., Srinivasan, P., Muthukumar, C.C., Wang, Role of hybrid nanofluid in heat transfer enhancement–A review, International Communications in Heat and Mass Transfer, Elsevier Ltd, 2021.

[27] A., Abdulrahman, F., Gamaoun, R.V., Kumar, U., Khan, H.S., Gill, K.V., Nagaraja, A.M., Galal, Study of thermal variation in a longitudinal exponential porous fin wetted with TiO_2 SiO_2/hexanol hybrid nanofluid using hybrid residual power series method, Case Studies in Thermal Engineering, Elsevier Ltd, Volume 43, 2023.

[28] B.J., Gireesha, G., Sowmya, M.I., Khan, H.F., Oztop, Flow of hybrid nanofluid across a permeable longitudinal moving fin along with thermal radiation and natural convection, Computer methods and programs in biomedicine, Elsevier Ltd, Volume 185, 2020.

[29] B.J., Gireesha, G., Sowmya, S., Sindhu, Analysis of thermal behavior of moving longitudinal porous fin wetted with water based SWCNTs and MWCNTs, Heat transfer, Wiley, 49(4), pp 2044 2058, 2020.

[30] C., Selvam, E.C.M., Irshad, D.M., Lal, S., Harish Experimental Thermal and Fluid Science, 2016, Convective heat transfer characteristics of water–ethylene glycol mixture with silver nanoparticles, Experimental Thermal and Fluid Science, Elsevier, Volume 77, pp 188 196, 2016.

[31] B.J., Gireesha, G., Sowmya, M.I., Khan, H.F., Oztop, Flow of hybrid nanofluid across a permeable longitudinal moving fin along with thermal radiation and natural convection, Computer methods and programs in biomedicine, Elsevier Ltd., Volume 185, 2020.

[32] K.K., Gupta, M., Ramachandran, Effect of Ethylene glycol as Phase Change Material in a Cold Storage Unit on retention of cooling, In IOP Conference Series: Materials Science and Engineering, IOP Publishing 377(1), 2018.

[33] P., Jalili, S.G., Alamdari, B., Jalili, A., Shateri, D.D., Ganji Heliyon, Analytical and numerical investigation of heat transfer of porous fin in a local thermal non equilibrium state, Heliyon, Elsevier Ltd, 10(4), pp 2405 8440, 2024.

[34] H., Mirgolbabaee, D.D., Ganji, S.T., Ledari, Heat transfer analysis of a fin with temperature dependent thermal conductivity and heat transfer coefficient, New Trends in Mathematical Sciences, BISKA Bili¸ sim Technology, 3(2), pp 55 69, 2015.

[35] H., Mirgolbabaee, D.D., Ganji, S.T., Ledari, an assessment of a semi analytical AG method for solving nonlinear oscillators, New Trends Math. Sci, BISKA Bili¸sim Technology, 4(1), pp 283 299, 2016.

[36] H., Mirgolbabaee, S.T., Ledari, D.D., Ganji, E.K., Valujai, Analyzing the nonlinear heat transfer equation by AGM, New Trends in Mathematical Sciences, BISKA Bili¸ sim Technology, 5(1), 51 58, 2017.

[37] G., Sowmya, B.J., Gireesha, O.D., Makinde, Thermal performance of fully wet longitudinal porous fin with temperature dependent thermal conductivity, surface emissivity and heat transfer coefficient. Multidiscipline Modeling in Materials and Structures, Emerald, 16(4), 749 764, 2020

[38] S., Hosseinzadeh, Hosseinzadeh, K., Hasibi, A., & Ganji, D. D. (2022). Thermal analysis of moving porous fin wetted by hybrid nanofluid with trapezoidal, concave parabolic and convex cross sections. Case Studies in Thermal Engineering, 30, 101757.